

T.33
1998

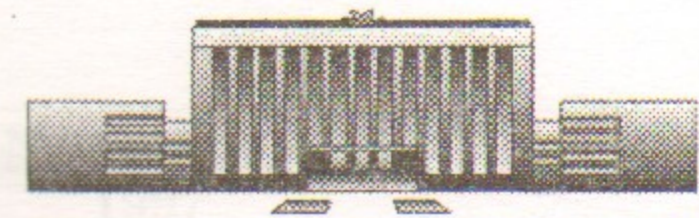
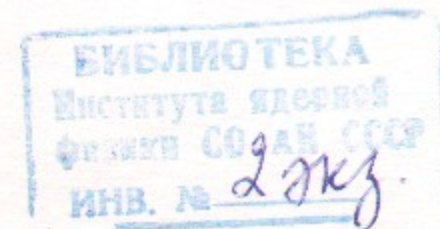


Budker Institute of Nuclear Physics
SB RAS

V.I. Telnov

**HIGH ENERGY
PHOTON-PHOTON COLLIDERS**

Budker INP 97-71



Novosibirsk

✓

High Energy Photon-Photon Colliders ¹

Valery Telnov

Budker Institute of Nuclear Physics,
630090 Novosibirsk, Russia

Abstract

Using the laser backscattering method at future TeV linear colliders one can obtain $\gamma\gamma$ and γe colliding beams (photon colliders) with the energy and luminosity comparable to that in e^+e^- collisions. Now this option is included to conceptual designs of linear colliders. This paper is a short introduction to this field with an emphasis on required lasers which can be used both for $e \rightarrow \gamma$ conversion and for preparation of electron beams (photoguns, laser cooling), some interesting nonlinear QED effects in a strong field which apply restrictions on parameters of photon colliders are discussed.

©Budker Institute of Nuclear Physics,
630090 Novosibirsk, Russia

¹Talk at XI International Vavilov's Conference on nonlinear optics Novosibirsk, June 24-28, 1997

1 Introduction

It is well known that according to Maxwell's equations electromagnetic waves in vacuum cross each other without perturbations. Quantum electrodynamics predicts nonzero cross section of photon-photon scattering (via box diagram with virtual e^+e^- pairs). However for the optical photons this cross section is extremely small, about 10^{-63} cm² growing very fast with the energy ($\propto \omega^6$ for $\omega \ll m_e c^2$). At high energies, photons can produce pairs of charged particles (e^+e^- , $\mu\mu$, ... $q\bar{q}$, WW etc.) and other final states.

Physics of elementary particles is studied in collisions of particles of various types: pp , $p\bar{p}$, ep , e^+e^- , etc..., which allows to produce new particles, investigate their properties, structure and interaction. Photon collisions are also of great interest. Photons, as electrons, are elementary particles (that is important for interpretation of results), cross sections of new particle production in photon-photon collisions are of the same order as that in e^+e^- collisions. Many phenomena of particle physics can be studied in $\gamma\gamma$ collision in the best way. Generally speaking, physics in $\gamma\gamma$ collisions is complimentary to that studied in other types of collisions. For example, e^+e^- annihilation goes via one virtual photon and resonances with odd charged parity (the same as for photon) are produced: $\rho_0, \phi, \dots \Psi, \Upsilon, Z$. While in $\gamma\gamma$ collisions resonances with even charged parity are produced: $\pi_0, \eta, \dots f, \eta_c, \chi, \dots H$.

Since 1970, two-photon physics has been actively studied at e^+e^- storage rings. An electromagnetic field of a relativistic charged particle is transverse and can be treated as equivalent photons. Approximately accuracy one can

Table 1: Some parameters of 0.5 TeV linear colliders, updated in 1996

project	TESLA	SBLC	JLC(X)	NLC	CLIC	VLEPP
country/center	Germany	Germany	Japan	USA	CERN	Russia
$L, 10^{33} \text{ cm}^{-2} \text{ s}^{-1}$	6	5.3	5.1	5.5	6.4	9.7
rep.rate, Hz	5	50	150	180	700	300
# bunch/train	1130	333	85	90	20	1
part./bunch(10^{10})	3.6	1.1	0.65	0.75	0.8	20
$\sigma_x(\text{nm})$	845	335	260	295	264	2000
$\sigma_y(\text{nm})$	19	15	3	6.3	5	4
$\sigma_z(\text{mm})$	0.7	0.3	0.09	0.125	0.16	0.75
Δt bunch(ns)	708	6	1.4	1.4	1	—

assume that each electron is accompanied by almost real photon with the probability $dn_\gamma \sim (\alpha/\pi) \ln \gamma^2 d\omega/\omega \sim 0.035 d\omega/\omega$. These experiments have given a lot of information on the nature of elementary particles. For example, it was found that some of known C-even mesons have very small cross sections in $\gamma\gamma$ collision that indicates that they have not quark-antiquark nature (as usually) but more likely they consist of four quark or two gluons.

However, the $\gamma\gamma$ luminosity (number of events/second is proportional to luminosity) in collisions of virtual photons at storage rings is much lower than e^+e^- luminosity and concentrated mainly in the region of low invariant masses of $\gamma\gamma$ system. In the region $W_{\gamma\gamma}/2E_0 > 0.5$ it accounts for only 0.02% of e^+e^- luminosity. Therefore, it is natural that most of discoveries were done in e^+e^- collisions.

Maximum energy of e^+e^- storage ring is about 100 GeV (LEP-II at CERN with circumference 27 km). Due to severe synchrotron radiation in storage rings the energy region beyond LEP-II can be explored only with linear colliders. Such linear colliders of 500 — 1500 GeV center-of-mass energy are developed now in the main high energy centers [1]. Some parameters of the linear colliders are presented in table 1. Parameters of electron beams here are optimized for e^+e^- collisions. The luminosity (L) of colliders given in the third line characterizes the rate of events and it is defined as follows: the number of events of a certain class per second $\dot{n} = L\sigma$, where σ is the cross section of the process. For cylindrical Gaussian beams $L \approx N^2 f / 4\pi\sigma_x\sigma_y$, where N is the number of particles in the beam, σ_x, σ_y are transverse beam sizes, f is the collision rate.

Linear colliders offer unique, much more rich than before, opportunities to study $\gamma\gamma$ and γe interactions. Unlike the situation in storage rings, in linear colliders each bunch is used only once. This makes it possible to "convert" electron to high energy photons to obtain colliding $\gamma\gamma$ and γe beams [2, 3]. Among various method of $\gamma \rightarrow e$ conversion the best one is Compton scattering of laser light on high energy electrons. The basic scheme of a photon collider is the following, fig.1. Two electron beams after the final focus system are traveling toward the interaction point (IP). At a distance of about 0.1–1 cm upstream from the IP, at the conversion point (C), the laser beam is focused and Compton backscattered by electrons, resulting in the high energy beam of photons. With reasonable laser parameters one can "convert" most of electrons into high energy photons. The photon beam follows the original electron direction of motion with a small angular spread of order $1/\gamma$, arriving at the IP in a tight focus, where it collides with the similar opposing high energy photon beam or with an electron beam. The photon spot size at the IP may be almost equal to that of electrons at IP and therefore, the luminosity of $\gamma\gamma, \gamma e$ collisions will be of the same order of magnitude as the "geometric" luminosity of basic ee beams.

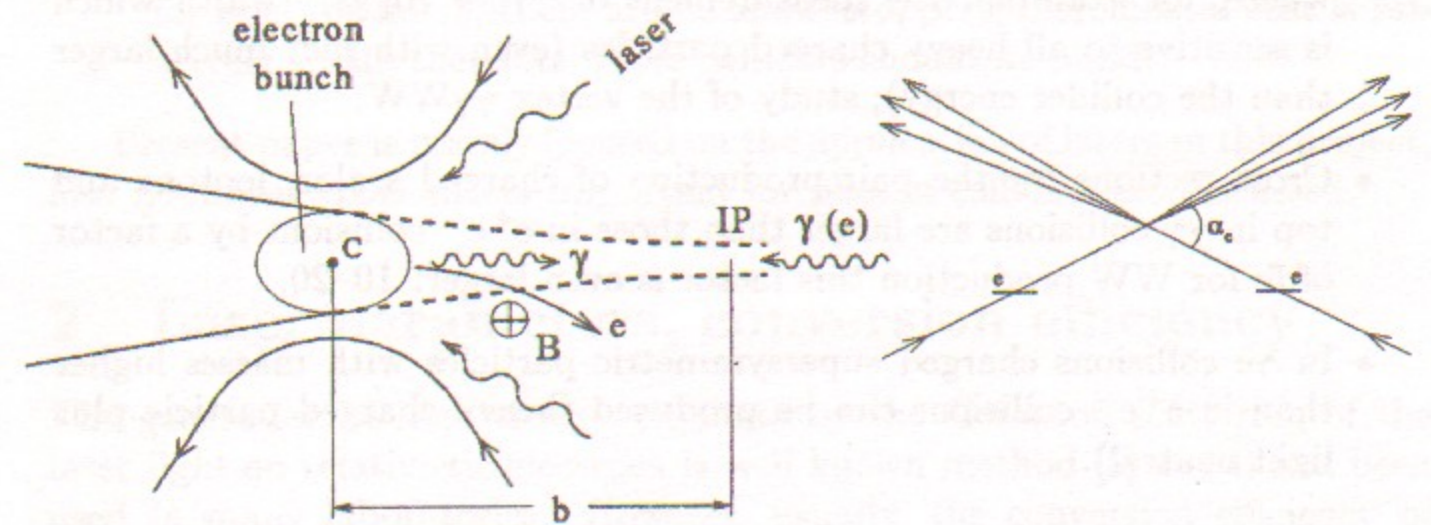


Figure 1: Scheme of $\gamma\gamma; \gamma e$ collider. Figure 2: Crab-crossing scheme.

Two collision scheme were considered. In the first scheme there is no magnetic deflection of spent electrons and all particles after the conversion region travel to the IP. The conversion point may be situated very close to the IP. In the second scheme after the conversion region particles pass through a region with a transverse magnetic field ($B \sim 0.5-1$ T) where electrons are swept aside. Thereby one can achieve more or less pure $\gamma\gamma$ or γe collisions.

In both schemes the removal of the disrupted spent beams (with very wide energy spread, $E = (0.02 - 1)E_0$, can best be done using the crab-crossing scheme, fig. 2. In this scheme the electron bunches are tilted (using RF cavity) with respect to the direction of the beam motion, and the luminosity is then the same as for head-on collisions. Due to the collision angle $\alpha_c \sim 30$ mrad the outgoing disrupted beams travel outside the final quads.

The detailed description of photon colliders properties can be found in refs [3]–[7] and in the Berkeley Workshop Proceedings [8]. Recently this option was included into the Conceptual Design Reports of the NLC [9], TESLA-SBLC [10] and JLC. All these linear collider projects foresee an interaction region for $\gamma\gamma, \gamma e$ collisions.

Physical problems, which can be studied in $\gamma\gamma$ and γe collisions, were discussed in hundred papers. Recent review of physics at photon colliders can be found, for example, in TESLA/SBLC Conceptual Design Report [10].

These studies of possible physics and technical problems have shown that photon colliders are quite realistic and can substantially add to a discovery potential of linear colliders. Below is some list of arguments in favor of photon colliders.

- Some phenomena can be studied at photon colliders better than anywhere, for example: the measurement of $\gamma\gamma \rightarrow \text{Higgs}^2$ width which is sensitive to all heavy charged particles (even with mc^2 much larger than the collider energy); study of the vertex $\gamma\gamma WW$.
- Cross sections for the pair production of charged scalar, leptons and top in $\gamma\gamma$ collisions are larger than those in e^+e^- collisions by a factor of 5; for WW production this factor is even larger: 10–20.
- In γe collisions charged supersymmetric particles with masses higher than in e^+e^- collisions can be produced (heavy charged particle plus light neutral).
- The luminosity of photon colliders (in the high energy part of luminosity spectrum) with electron beam parameters considered in the present designs will be about $10^{33} \text{ cm}^{-2}\text{s}^{-1}$ or by a factor 5 smaller than $L_{e^+e^-}$. But the absence of collisions effects at 0.1 – 1 TeV photon colliders allows to reach $L_{\gamma\gamma}$ up to $10^{35} \text{ cm}^{-2}\text{s}^{-1}$ using electron beams with very

²Higgs boson (H) is undiscovered particle predicted in the unified theory of electroweak interactions, responsible for origin of particle masses. Its mass is not predicted in the theory, but from indirect experiments follows that $80 \text{ GeV} < M_H c^2 < 400 \text{ GeV}$, that is accessible for $p\bar{p}$ storage rings and linear e^+e^- , e^-e^- , γe , $\gamma\gamma$ colliders.

low emittances. High luminosity photon colliders can provide much higher production rate of WW pair and other charged particles than in e^+e^- collisions (see item 2).

- Obtaining of the ultimately high luminosities requires the development of new techniques, such as the laser cooling of electron beams [12]. However, linear colliders will appear (may be) only in one decade and will work next two decades. The upgrading of the luminosity requires the injection part modification only; it may be a separate injector for a photon collider, merging of many low emittance RF-photoguns (with or without laser cooling) is one of possible variants. Note that for photon colliders positron beams are not required that simplifies the task.
- Development of X-ray FEL lasers based on linear colliders (which are now under way) will favour the work on FEL required for photon colliders.
- Summarizing we can say that physics goals for $\gamma\gamma, \gamma e$ colliders are significant and complimentary to those in e^+e^- collisions; the technology (laser etc.) is sufficiently advanced and no more difficult or risky than for e^+e^- colliders, there are no show-stoppers; incremental cost is relatively small; therefore $\gamma\gamma, \gamma e$ colliders should be build.

Present paper is mainly focused on the application of lasers in this project, also nonlinear QED effects important for photon colliders are discussed.

2 Laser parameters, conversion efficiency

The generation of high energy γ -quanta by the Compton scattering of the laser light on relativistic electrons is well known method [5] and it has been used in many laboratories. However, usually, the conversion efficiency of electron to photons $k = N_\gamma/N_e$ is very small, only about 10^{-7} – 10^{-5} . At linear colliders, due to small bunch sizes one can focus the laser more tightly to the electron beams and get $k \sim 1$ at rather moderate laser flash energy.

In the conversion region, a laser photon with an energy ω_0 collides almost head-on with a high energy electron of the energy E_0 . The energy of the scattered photon ω depends on its angle ϑ with respect to the motion of the incident electron as follows [3]:

$$\omega = \frac{\omega_m}{1 + (\vartheta/\vartheta_0)^2}, \quad \omega_m = \frac{x}{x+1} E_0; \quad \vartheta_0 = \frac{mc^2}{E_0} \sqrt{x+1}; \quad (1)$$

where

$$x = \frac{4E\omega_0}{m^2c^4} \simeq 15.3 \left[\frac{E_0}{\text{TeV}} \right] \left[\frac{\omega_0}{\text{eV}} \right] = 19 \left[\frac{E_0}{\text{TeV}} \right] \left[\frac{\mu\text{m}}{\lambda} \right], \quad (2)$$

ω_m is the maximum energy of scattered photons. For example: $E_0 = 250$ GeV, $\lambda = 1.06 \mu\text{m}$, (Nd:Glass laser) $\Rightarrow x=4.5$ and $\omega/E_0 = 0.82$. The energy of the backscattered photons grows with x . The spectrum also becomes narrower. However, at $x > 2(\sqrt{2} + 1) \approx 4.8$ high energy photons are lost due to e^+e^- creation in the collisions with laser photons [3, 6, 7]. For example, at $x \sim 10$, the maximum effective conversion coefficient is $k_{max} \sim 0.3$, while at $x < 4.8$ it can be about 0.65 (one conversion length) or even high. The luminosity is proportional to k^2 and in the latter case it is larger by a factor of 5. So, the value $x \sim 4.8$ is optimum, though higher x are also of interest for the experiments where the ultimate monochromaticity of $\gamma\gamma$ collisions is required. The wave length of the laser photons corresponding to $x = 4.8$ is

$$\lambda = 4.2E_0[\text{TeV}] \mu\text{m}. \quad (3)$$

For $2E_0 = 500$ GeV it is about $1 \mu\text{m}$, that is the region of the most powerful solid state lasers. The energy spectrum of the scattered photons for $x = 4.8$ is shown in fig. 3 for various helicities of the electron and laser beams (here λ_e is the mean electron helicity ($|\lambda_e| \leq 1/2$), P_c is the helicity of laser photons. We see that with the polarized beams at $2\lambda_e P_c = -1$ the number of high energy photons is nearly double. The spectrum in fig. 3 corresponds to the case of small conversion efficiency. In the thick target each electron may undergo the multiple Compton scattering. The secondary photons are softer in general and populate the low energy part of the spectrum. If a laser light is polarized, high energy photons are also polarized. Corresponding curves can be found elsewhere [4, 7]. The polarization is very advantageous for many experiments.

The spectrum of scattered photons is very broad, but because of energy-angle correlation in the Compton scattering it is possible to obtain rather narrow distributions of the spectral luminosities in $\gamma\gamma$ and γe collisions. Spectral luminosity distributions depend on the variable $\rho = b/\gamma a$, where b is the distance between the conversion region and the interaction point (i.p.), a is the r.m.s. radius of the electron beam at the i.p.. If $\rho \ll 1$, then at i.p. photons of various energies collide with each other and the distribution in the invariant mass of $\gamma\gamma$ or γe system is broad. But, if $\rho \gg 1$, then in γe collisions electrons collide only with the highest energy photons, therefore the invariant mass spectrum of γe collision is narrow. In $\gamma\gamma$ collisions at $\rho \gg 1$ the photons with higher energy collide at smaller spot size and, therefore,

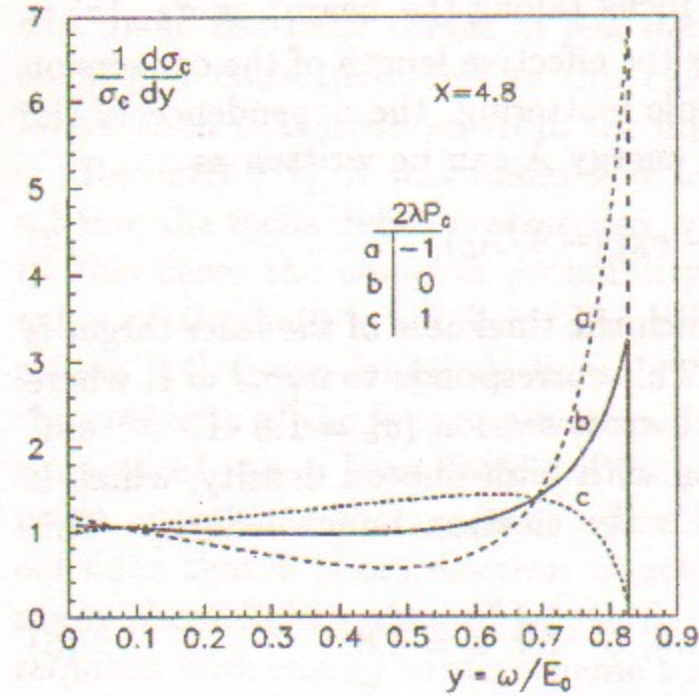


Figure 3: Spectrum of the Compton scattered photons for various polarizations of laser and electron beams.

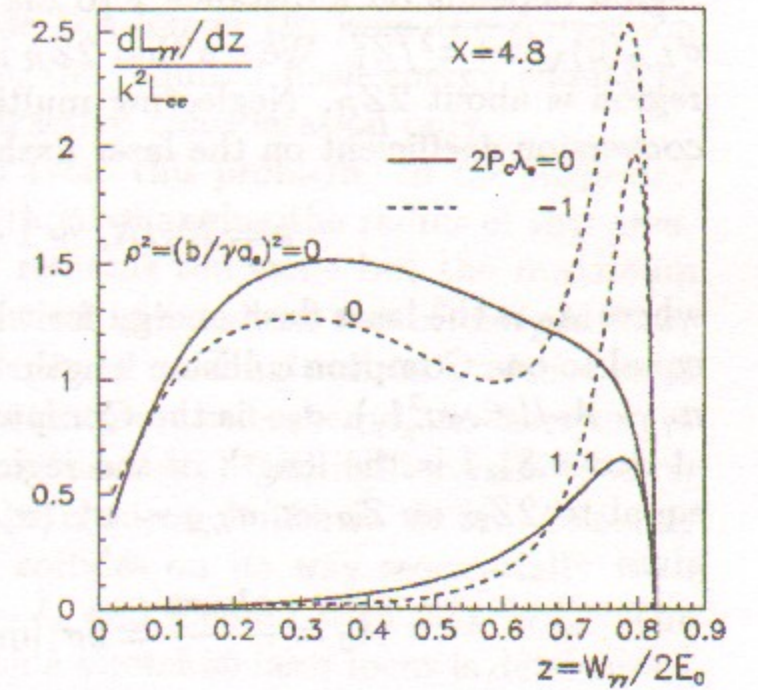


Figure 4: Spectral luminosity of $\gamma\gamma$ collisions, see comments in the text.

contribute more to the luminosity. As a result, the luminosity spectrum is much narrower than at $\rho \ll 1$. In fig. 4 the plots of spectral $\gamma\gamma$ luminosities are shown in collisions of round beams at a low conversion coefficient. The cases of unpolarized and polarized beams ($2P_e \lambda_e = -1$ both beams) for $\rho = 0$ and 1 are presented [7]. One can see that at $\rho = 1$ the luminosity in the low mass region is strongly suppressed and the full width at half of maximum is about 10% for polarized and 20% for unpolarized beams. In realistic cases one should take into account photons from the multiple Compton scattering and emitted by electrons in the strong field of the opposing beam (so called "beamstrahlung"), examples of realistic luminosity distribution can be found elsewhere [7, 10].

A laser flash energy required for obtaining conversion efficiency close to 100% can easily be estimated using well known characteristics of a laser beam with diffraction divergence. The emittance of the Gaussian laser bunch with diffraction divergence is $\epsilon_{x,y} = \lambda/4\pi$. The r.m.s. spot size of a laser beam at the focus ($i = x, y$) [3], $\sigma_{L,i}(0) = \sqrt{\lambda Z_R/4\pi}$, where Z_R is known as the Rayleigh length. The r.m.s. transverse size of a laser near the conversion

region depends on a distance z to the focus (along the beam) as $\sigma_{L,x}(z) = \sigma_{L,x}(0)\sqrt{1+z^2/Z_R^2}$. We see that $2Z_R$ is the effective length of the conversion region is about $2Z_R$. Neglecting multiple scattering, the dependence of the conversion coefficient on the laser flash energy A can be written as

$$k = N_\gamma/N_e \sim 1 - \exp(-A/A_0), \quad (4)$$

where A_0 is the laser flash energy for which the thickness of the laser target is equal to one Compton collision length. This corresponds to $n_\gamma\sigma_c l = 1$, where $n_\gamma \sim A_0/(\pi\omega_0 a_\gamma^2 l_\gamma)$, σ_c - is the Compton cross section ($\sigma_c = 1.8 \cdot 10^{-25}$ cm² at $x = 4.8$), l is the length of the region with high photon density, which is equal to $2Z_R$ at $Z_R \ll \sigma_{L,z} \sim \sigma_z$ (σ_z is the electron bunch length). This gives

$$A_0 = \frac{\pi\hbar c\sigma_z}{\sigma_c} = 5\sigma_z[\text{mm}], \quad J \quad \text{for } x = 4.8. \quad (5)$$

Note, that the required flash energy decreases with reducing the Rayleigh length down to σ_z , and it is hardly changed with further decrease in Z_R . This is because the density of photons grows but the length having a high density decreases and the Compton scattering probability remains almost the same. It is not helpful to make the radius of the laser beam at the focus smaller than $\sigma_{L,x} \sim \sqrt{\lambda\sigma_z/4\pi}$, which may be much larger than the transverse electron bunch size at the conversion region.

Above we have considered only the geometrical properties of the laser beam and the pure Compton effect. However, in the strong electromagnetic field at the laser focus, multiphoton effects (non-linear QED) are important. Nonlinear effects are described by the parameter [11]

$$\xi^2 = (eB\hbar/m\omega_0 c)^2, \quad (6)$$

where B is the r.m.s. strength of the magnetic field in the laser wave. At $\xi^2 \ll 1$ an electron interacts with one photon (Compton scattering), while at $\xi^2 \gg 1$ an electron scatters on many laser photons simultaneously (synchrotron radiation in a wiggler). The transverse motion of an electron in the electromagnetic wave leads to an effective increase in the electron mass: $m^2 \rightarrow m^2(1 + \xi^2)$, and the maximum energy of scattered photons decreases: $\omega_m = x/(1 + x + \xi^2)$. At $x = 4.8$, the value of ω_m/E_0 decreases by 10% at $\xi^2 = 0.6$. Although this can be compensated by some increase in x , but, in any case, large ξ^2 leads to smearing of the high energy Compton peak. The value of $\xi^2 \sim 1$ can be considered as the limit.

The nonlinear QED effects are more important for projects with shorter bunches and higher beam energies (larger λ) and makes problems already for

some current projects [6, 7]. In principle, in order to avoid this problem one can make the laser target of less dense but longer (to keep the conversion coefficient constant). But in this case, the required flash energy should be larger than that deduced from the diffraction consideration only.

Recently [12], it was found how to avoid this problem. In the suggested scheme the focus depth is stretched without changing the radius of this area. In this case, the collision probability remains the same but the maximum value of the field is smaller. The solution is based on use of chirped laser pulses [14] (wave length is linearly depends on longitudinal position) and chromaticity of the focusing system. In the proposed scheme, the laser target consists of many laser focal points (continuously) and light comes to each point exactly at the moment when the electron bunch is there. One can consider that a short electron bunch collides on its way sequentially with many short light pulses of length $l_\gamma \sim l_e$ and focused with $2Z_R \sim l_e$. The required flash energy in the scheme with a stretched laser focus is determined only by diffraction and at the optimum wave length does not depend on the collider energy.

3 Lasers

For conversion of electrons to photons with $k \sim 65\%$ at $x = 4.8$ and $E_0 = 250$ GeV a laser with the following parameters is required:

Power	$P \sim 0.7$ TW	Duration	$\tau(\text{rms}) \sim \sigma_z/c \sim 1 - 2.5$ ps
Flash energy	1 - 4 J	Rep. rate	$\sim 10^4$
Average power	~ 25 kW	Wave length	$\lambda = 4.2E0[\text{TeV}], \mu\text{m}$

Obtaining of such parameters is possible with solid state or free electron lasers (FEL). For $\lambda \geq 1\mu\text{m}$ ($E_0 > 250$ GeV) FEL is the only option seen now.

3.1 Solid state lasers

In the last ten years the technique of short powerful lasers made an impressive step and has reached petowatt (10^{15}) power levels and few femtosecond durations [13]. Obtaining few joule pulses of picosecond duration is not a problem. For photon collider applications the main problem is a high repetition rate. This is connected with overheating of the amplifying media.

The success in obtaining picosecond pulses is connected with a chirped pulse amplification (CPA) technique [14]. The principle of CPA is the following. A short, low energy pulse is generated in an oscillator. Then this pulse is stretched by a factor about 10^4 in the grating pair which has de-

lay proportional to the frequency. This long nanosecond pulse is amplified and compressed by another grating pair to a pulse with the initial or somewhat longer duration. Due to practical absence of non-linear effects for the stretched pulses, the obtained pulses have a very good quality close to the diffraction limit.

One of such lasers [15] works now in the E-144 experiment studying non-linear QED effects in the collision of laser photons and 50 GeV electrons. It has a repetition rate of 0.5 Hz, $\lambda = 1.06 \mu\text{m}$ (Nd:Glass), 2J flash energy, 2 TW power and 1 ps duration. This is a top-table laser with flash lamp pumping. Its parameters are very close to our needs, only the repetition rate is too low. Further progress in the repetition rate (by two orders) is possible with a diode pumping (high efficiency semiconductor lasers). With diode pumping the efficiency of solid state lasers reaches a 10% level. Recent studies [15, 16, 9] have shown that the combination of CPA, diode pumping, zig-zag slab amplifier, recombining of several lasers (using polarizers and Pockel cells or slightly different wave lengths), and other laser techniques (if necessary) such as phase-conjugated mirrors, moving amplifiers allows already now to build a solid state laser system for a photon collider. All necessary technologies are developing actively now for other applications.

3.2 Free electron lasers

Free electron lasers (FEL) are very attractive for gamma-gamma collider. Indeed, FEL radiation is tunable and has always minimal (i.e. diffraction) dispersion. The FEL radiation is completely polarized: circularly or linearly for the case of helical or planar undulator, respectively. The problem of synchronization of the laser and electron bunches at the conversion region is solved by means of conventional methods used in accelerator techniques. A FEL amplifier has potential to provide high conversion efficiency of the kinetic energy of an electron beam into coherent radiation, up to 10%. At sufficient peak power of the driving electron beam the peak power of the FEL radiation could reach the required TW level. A short review of activities on FEL for photon colliders and references can be found elsewhere [10].

4 Optics at the interaction region

The possible layout of optics near the IP is shown in fig. 5 [10]. The conversion region is situated at a distance $b \sim 1.5\gamma\sigma_y = 0.5\text{--}1.5 \text{ cm}$ from the IP. Beams collide at the IP at the crab-crossing angle 30 mrad (see fig. 2).

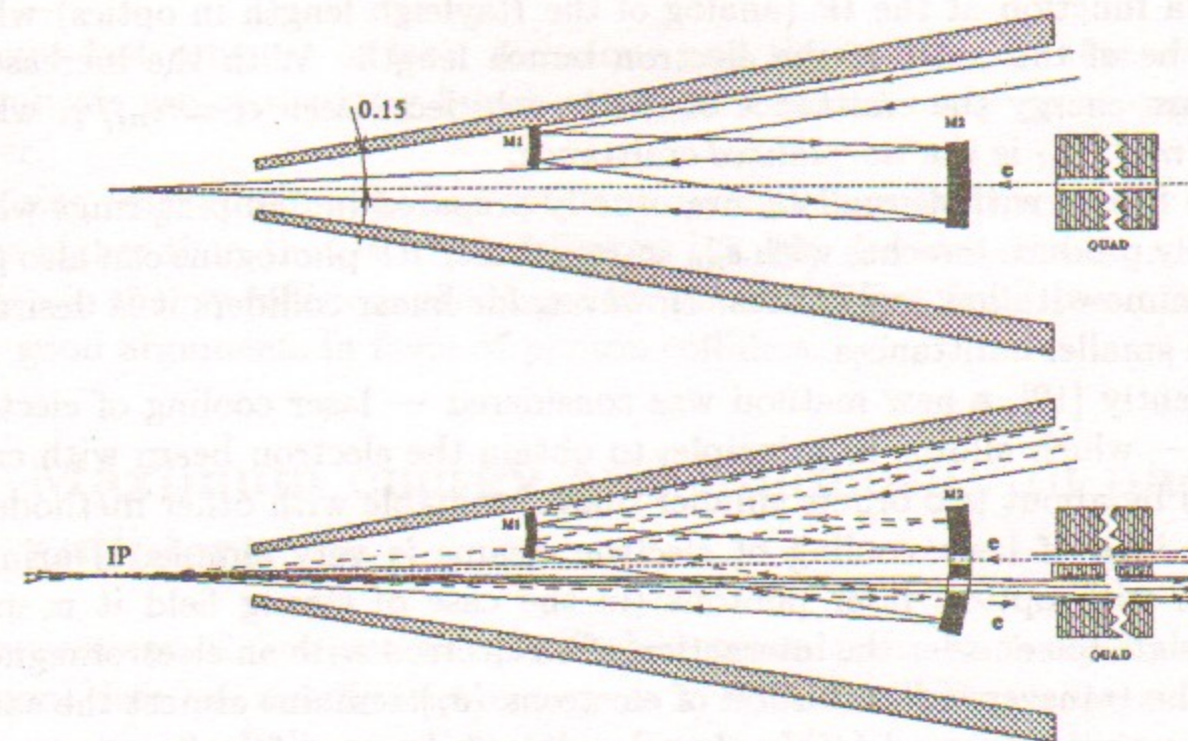


Figure 5: Layout of laser optics near the IP; upper - side view, down - top view, dashed lines - exit path of light coming from the left through one of the CP points (right to the IP), the distance between the IP and quads is about 2 m

The distance between IP and final quad is about 2 m. All the optics is situated inside a tungsten conical mask which absorbs particle from showers on mirrors and quads. Arguments for choosing this geometry and estimation of mirror resistance are given in ref. [10].

5 Laser cooling

To attain high luminosity, beams in linear colliders should be very tiny. At the interaction point (IP) in the current LC designs [1], beams with transverse sizes as low as $\sigma_x/\sigma_y \sim 200/4 \text{ nm}$ are planned. Beams for e^+e^- collisions should be flat in order to reduce beamstrahlung energy loss (synchrotron radiation in the field of the opposing beam). For $\gamma\gamma$ collision, the beamstrahlung radiation is absent and beams with smaller σ_x can be used to obtain higher luminosity.

The transverse beam sizes are determined by the emittances ϵ_x , and ϵ_y . The beam sizes at the interaction point (IP) are $\sigma_i = \sqrt{\epsilon_i \beta_i}$, where β_i is

the beta function at the IP (analog of the Rayleigh length in optics) which should be of the order of the electron bunch length. With the increase in the beam energy the emittance of the bunch decreases: $\epsilon_i = \epsilon_{ni}/\gamma$, where $\gamma = E/mc^2$, ϵ_{ni} is the *normalized* emittance.

The beams with a small ϵ_{ni} are usually prepared in damping rings which naturally produce bunches with $\epsilon_{ny} \ll \epsilon_{nx}$. Laser RF photoguns can also produce beams with low emittances. However, for linear colliders it is desirable to have smaller emittances.

Recently [12], a new method was considered — laser cooling of electron beams — which allows, in principle, to obtain the electron beam with cross sections by about two orders smaller than attainable with other methods.

The idea of laser cooling of electron beams is very simple. During a collision with optical laser photons (in the case of strong field it is more appropriate to consider the interaction of an electron with an electromagnetic wave) the transverse distribution of electrons (σ_i) remains almost the same. Also, the angular spread (σ'_i) is almost constant, because for photon energies (a few eV) much lower than the electron beam energy (several GeV) the scattered photons follow the initial electron trajectory with a small additional spread. So, the emittance $\epsilon_i = \sigma_i \sigma'_i$ remains almost unchanged. At the same time, the electron energy decreases from E_0 down to E . This means that the transverse normalized emittances have decreased: $\epsilon_n = \gamma \epsilon = \epsilon_{n0}(E/E_0)$. One can reaccelerate the electron beam up to the initial energy and repeat the procedure. Then after N stages of cooling $\epsilon_n/\epsilon_{n0} = (E/E_0)^N$ (if ϵ_n is far from its limit).

Some possible sets of parameters for the laser cooling are: $E_0 = 4.5$ GeV, $l_e = 0.2$ mm, $\lambda = 0.5$ μ m, flash energy $A \sim 10$ J. The final electron bunch will have an energy of 0.45 GeV with an energy spread $\sigma_E/E \sim 13\%$, the normalized emittances $\epsilon_{nx}, \epsilon_{ny}$ are reduced by a factor 10. A two stage system with the same parameters gives 100 times reduction of emittances. The limit on the final emittance is $\epsilon_{nx} \sim \epsilon_{ny} \sim 2 \times 10^{-9}$ m rad. For comparison, in the TESLA (NLC) project the damping rings have $\epsilon_{nx} = 14(3) \times 10^{-6}$ m rad, $\epsilon_{ny} = 25(3) \times 10^{-8}$ m rad. The electron beam after laser cooling accelerated to one TeV energy can be focused to a spot with about 0.5 nm diameter.

For obtaining ultimate emittances the parameter ξ^2 in the cooling region should be less than one (Compton scattering) [12]. This is also necessary for preserving the electron polarization. These conditions can be achieved using the method of laser focus stretching described in sect.2.

Laser cooling requires a laser system even more powerful than that for $e \rightarrow \gamma$ conversion. However, all the requirements are reasonable taking into

account fast progress of laser technique and time plans of linear colliders. A multiple use of the laser bunch can reduce considerably an average laser power.

Using laser cooling one can attain in $\gamma\gamma$ collisions the luminosity by one order higher than that in e^+e^- collisions [17, 18]. Besides, the typical cross section in the $\gamma\gamma$ collisions are larger by a factor of five. Both these facts are very good arguments in favor of photon colliders.

6 Maximum energy and luminosity of photon colliders

Cross sections of “interesting” physical processes (such as charged pair production) decrease usually with energy as $1/E_{cm}^2$, where E_{cm} is the center-of-mass energy of colliding particles, therefore the luminosity of colliders should grow proportionally to E_{cm}^2 . A reasonable scaling for the required $\gamma\gamma$ luminosity at $\gamma\gamma$ collider is

$$L_{\gamma\gamma} \sim 3 \times 10^{33} E_{cm}^2 \text{ cm}^{-2}\text{s}^{-1}, \quad (7)$$

where E_{cm} is in TeV unit. In e^+e^- collisions characteristic cross sections are somewhat smaller and a required luminosity is larger by a factor of 5.

In linear colliders, each bunch is used only once, its production and acceleration requires a certain power. It means that the number of accelerated particle can not be increased with energy. In current projects a power consumption is already 100–200 MW. The only way to increase the luminosity is a decrease in transverse beam sizes at the interaction point.

In e^+e^- collision, the minimum beam sizes are determined by strong radiation of particles in the field of the opposing beam (beamstrahlung) and beam-beam instability. These effects impose strong restrictions on beam parameters and determine the attainable luminosity in e^+e^- collisions. In table 1 one can see that all projects use the flat beams, vertical size is of the order of 3–20 nm and horizontal size is larger by a factor of 100. This is because for the same beam cross section the electromagnetic field is reverse proportional to the largest transverse size.

6.1 Restrictions due to coherent pair creation

At the first sight, in $\gamma\gamma$ collisions both beams are neutral and collision effects should be absent. It is not a case. The conversion point is situated very close

to the interaction point (IP), and electrons after conversion pass the IP very close to the axis and influence on the oncoming photons and electrons.

What happens with photons? First of all, a photon can be converted into e^+e^- pair in a collision with an individual electron (Bethe-Heitler process — incoherent pair creation). The cross section of this process at high energies is about $4 \times 10^{-26} \text{ cm}^2$. The characteristic luminosity in one bunch collision is about $10^{30} \text{ cm}^{-2}\text{s}^{-1}$ therefore as much as $10^4 e^+e^-$ pairs will be produced per one bunch collisions (these pairs move in forward direction and do not cause serious background in detector). Note, that this process does not destroy the beam containing about 10^{10} photons.

More important for photon colliders is the process of *coherent pair creation* (conversion of a photon into e^+e^- pair in the collective field of an opposing electron beam) [19, 6, 7, 17]. This process becomes important for the beam fields B ($|E| + |B|$ in our problem) when $\kappa = (\omega/mc^2)/(B/B_0) > 1$, where $B_0 = m^2c^3/e\hbar = \alpha e/r_e^2 = 4.4 \times 10^{13} \text{ G}$ is the critical field, $r_e = e^2/mc^2$ is the classical radius of electron, ω is the photon energy. The origin of this condition is the following. In the rest system of the virtual e^+e^- pair created by the photon the electrical field of the beam is $E' = (\omega/mc^2) \times B$. If the energy acquired by e^+ and e^- in this field on the Compton wave length $\lambda_c = \hbar/mc$ is larger than mc^2 then a virtual particle may become a real one. That is a spontaneous pair creation in a strong field. In our problem the field of the opposing beam in the reference system of the oncoming beam can exceed the critical field $B_0 = 4.4 \times 10^{13} \text{ G}$. So, the critical field can be exceeded not only in stars but also at high energy linear colliders.

The coherent pair creation can impose restriction on the value of attainable luminosity. Fortunately, at an energy below about one TeV (which is a goal of the next linear colliders) this effect is considerably suppressed due to repulsion of electron beams during collisions. Even infinitely narrow electron beams after repulsion at the IP create an acceptable field on the axis, which does not cause catastrophic loss of the $\gamma\gamma$ luminosity.

Some simulation results of the attainable $\gamma\gamma$ luminosity are shown in fig. 6[17]. It was assumed that the conversion point is situated as close as possible to the IP at a distance $b = 3\sigma_z + 0.04E[\text{TeV}] \text{ cm}$. The second number is equal to the minimum length of the conversion region posed by nonlinear QED effects. The vertical electron beam size was taken smaller than b/γ , the horizontal size was varied. The total beam power was kept equal to $15E_{cm}[\text{TeV}] \text{ MW}$. In fig. 6 one can see that, if the collision effects are not important, the luminosity curves follow their natural behavior $L \propto 1/\sigma_x$. This is valid for all curves at large horizontal beam sizes (low beam fields). At low σ_x some curves make zigzag or change slope, this is due to the conversion

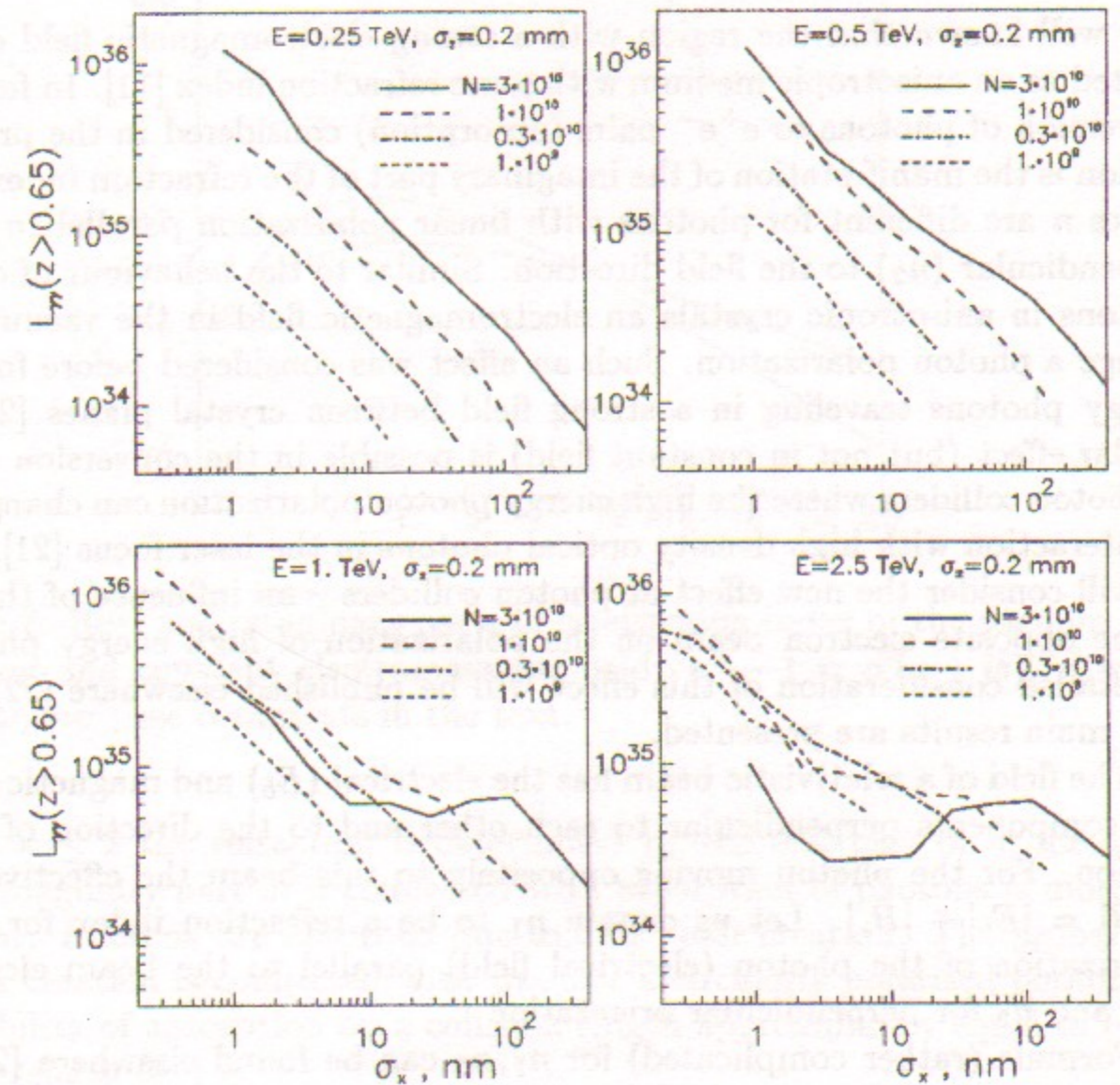


Figure 6: Dependence of the $\gamma\gamma$ luminosity on the horizontal beam size for $\sigma_z = 0.2 \text{ mm}$, see comments in the text.

of photons into e^+e^- pairs.

These results lead us to following conclusions. For the energies $E_{cm} < 2 \text{ TeV}$, which are in reach of the next generation of linear colliders, the luminosity limit is much higher than that required by our scaling for luminosity given by eq. 7. The energy limit for photon colliders is about $E_{cm} \sim 5\text{--}10 \text{ TeV}$.

6.2 Depolarization of photons in a strong beam field

It is well known that the region with a strong electromagnetic field can be treated as an anisotropic medium with some refraction index [11]. In fact, the conversion of photons to e^+e^- pairs (absorption) considered in the previous section is the manifestation of the imaginary part of the refraction index. The values n are different for photons with linear polarization parallel (n_1) and perpendicular (n_2) to the field direction. Similar to the behaviour of optical photons in anisotropic crystals an electromagnetic field in the vacuum can change a photon polarization. Such an effect was considered before for high energy photons traveling in a strong field between crystal planes [20]. A similar effect (but not in constant field) is possible in the conversion region at photon colliders where the high energy photon polarization can change due to interaction with high density optical photons in the laser focus [21]. Here we will consider the new effect at photon colliders – an influence of the field of the opposite electron beam on the polarization of high energy photons. A detailed consideration of this effect will be published elsewhere [22], here only main results are presented.

The field of a relativistic beam has the electrical (E_b) and magnetic ($B_b \approx E_b$) components perpendicular to each other and to the direction of beam motion. For the photon moving oppositely to this beam the effective field is $|B| = |E_b| + |B_e|$. Let us denote n_1 to be a refraction index for linear polarization of the photon (electrical field) parallel to the beam electrical field and n_2 for perpendicular orientation.

Formula (rather complicated) for n_1, n_2 can be found elsewhere [23, 24, 25]. It can be written in the form

$$n_i^2 - 1 = \alpha(a_i + ib_i)/\gamma^2, \quad (8)$$

where $\alpha = e^2/\hbar c = 1/137$, $\gamma = \hbar\omega/mc^2$, a_i and b_i ($i = 1, 2$) are the functions of the parameter

$$\kappa = \gamma \frac{B}{B_0}, \quad (9)$$

where $B_0 = m_e^2 c^3 / e\hbar = \alpha e / r_e^2 = 4.4 \times 10^{13}$ G is the critical field. Values of a_i and b_i are plotted in fig. 7. Asymptotic values of n_i are the following

$$n_{1,2} - 1 \approx \begin{cases} \frac{\alpha}{\gamma^2} \left(\frac{11 \mp 3}{180\pi} \kappa^2 + i\sqrt{\frac{3}{2}} \frac{3 \mp 1}{32} \kappa e^{-8/3\kappa} \right), & \kappa \ll 1 \\ \frac{\alpha}{\gamma^2} \left(-\frac{5 \mp 1}{56\pi^2} \sqrt{3} \Gamma^4(2/3) (1 - i\sqrt{3}) (3\kappa)^{2/3} \right), & \kappa \gg 1 \end{cases} \quad (10)$$

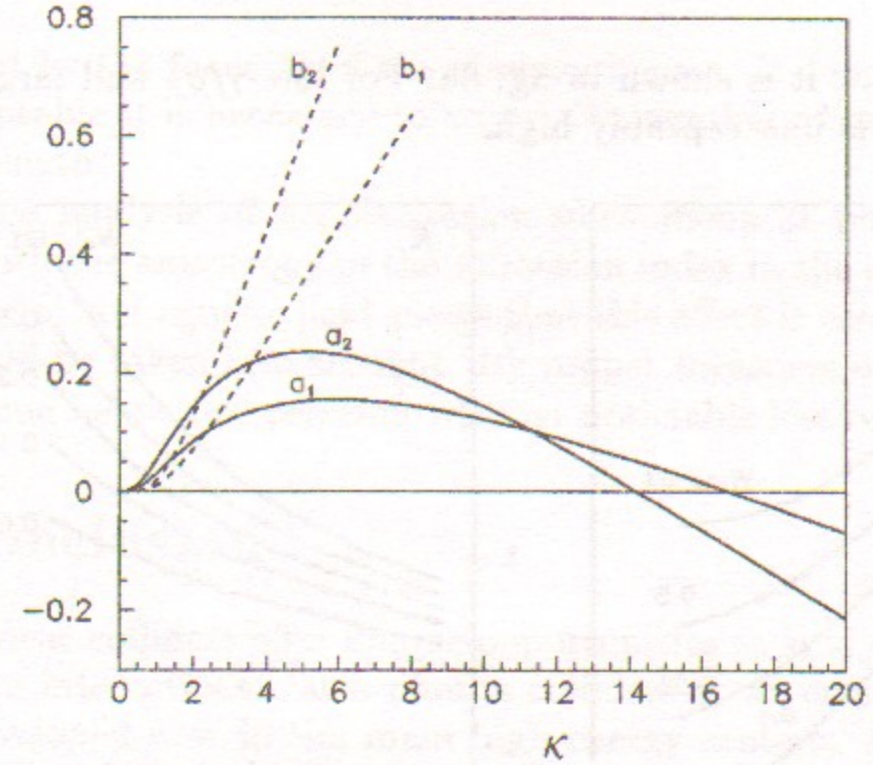


Figure 7: Real and imaginary parts of a refraction index of the vacuum with a strong and constant electromagnetic field: $n^2 - 1 = \alpha(a + ib)/\gamma^2$, where $\gamma = \hbar\omega/mc^2$; see comments in the text.

At $\kappa \leq 2$ the refraction is determined by the real part of n , for larger κ an imaginary part of n connected with absorption of photons is more important. Photons are absorbed due to e^+e^- pair creation. The probability of pair creation is connected with $\Im n$. For a circularly polarized photon the probability of absorption on a collision length approximately equal to r.m.s. bunch length (σ_z) is

$$W_{e^+e^-} \approx \alpha^2 \bar{b}(\kappa) \sigma_z / \gamma r_e. \quad (11)$$

We see that the beam field is an isotropic medium with different refraction indices for linear polarization parallel and perpendicular to the beam direction. Such a medium transforms the circular γ quanta polarization of into the linear polarization and vice versa. In addition, due to the difference in the absorption length the total polarization decreases. Using eqs. 8,11 one can obtain the decrease in circular polarization λ_γ during the beam collision (it is assumed that the initial polarization was 100%)

$$\frac{\Delta\lambda_\gamma}{\lambda_\gamma} = \frac{\alpha^4}{8\gamma^2} \left(\frac{\sigma_z}{r_e} \right)^2 (\Delta a^2 + \Delta b^2) = \frac{\Delta a^2 + \Delta b^2}{8b^2} W_{e^+e^-}^2, \quad (12)$$

here $\Delta a = a_2 - a_1$, $\Delta b = b_2 - b_1$, a and b are functions of κ . By excluding (numerically) κ from eqs. 11,12 we can find $\Delta\lambda_\gamma/\lambda_\gamma$ as a function of γ/σ_z

for different $W_{e^+e^-}$, it is shown in fig. 8a. For low γ/σ_z and large $W_{e^+e^-}$ the depolarization is unacceptably high.

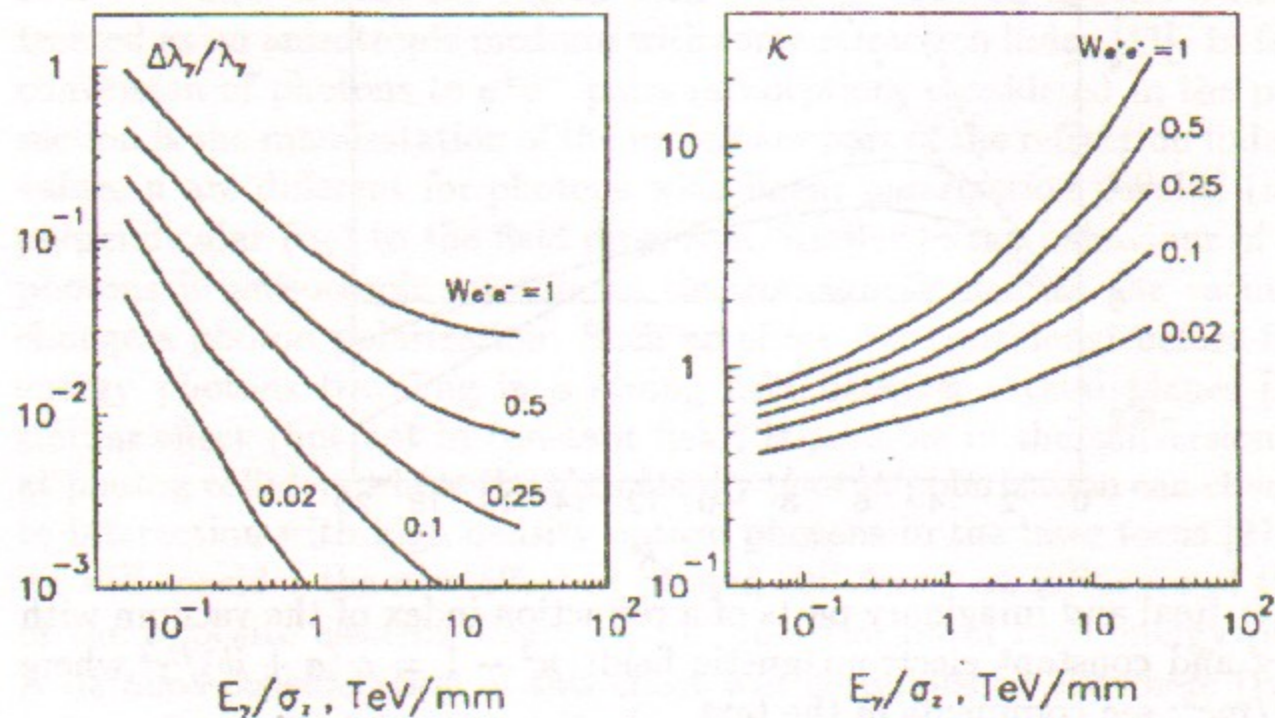


Figure 8: a) Decrease in a photon helicity during beam collisions for various beam parameters and probabilities of coherent pair creation (W); b) the parameter $\kappa = \gamma B/B_0$ for the conditions corresponding to the left figure. The luminosity at fixed value of abscissa is approximately proportional to $\kappa \times e^{-W}$, see additional comments in the text.

The e^+e^- pair creation is the only one effect restricting the $\gamma\gamma$ luminosity. In principle, it may happen that photons lose their polarization at the luminosity much lower than its limit posed by the pair creation. To check this we plotted in fig. 8b the values of κ as a function of the same parameters as those in fig. 8a. In order to decrease $\Delta\lambda_\gamma/\lambda_\gamma$ at fixed γ/σ_z we have to decrease $W_{e^+e^-}$ (see fig. 8a) which can be done, for example, by increasing the horizontal beam size σ_x . This corresponds to some decrease in κ (see fig. 8b). Now we can estimate the luminosity loss in this procedure. The luminosity is $L \propto (1/\sigma_x\sigma_y) \times e^{-W} \propto \kappa \times e^{-W}$. Looking at fig. 8b one can find that the retention of depolarization below 1% is accompanied by a very small loss of luminosity (compared to the maximum one), it is less than 20% in the whole region of parameters. This is very good. Note, however, that so simple adjustments of polarization loss by varying the horizontal beam size σ_x is not always possible. In the case where the initial electron beams are very narrow and the pair creation is suppressed only due to the beam repulsion (as it was discussed in the previous section) we will get some value of κ which is not

controlled by the focusing of the electron beams. If depolarization degree is not acceptable it is necessary to adjust the number of particles in the beam and its length.

So, the analysis of depolarization phenomena at photon colliders connected with the anisotropy of the refraction index in the collision region with a strong electromagnetic field shows that this effect is essential in some cases and should be taken into account. By proper measures one can keep the depolarization below few percents without noticeable loss of the $\gamma\gamma$ luminosity.

7 Conclusion

Future linear colliders offer unique opportunities to study particle physics in $\gamma\gamma$ and γe interactions. Such photon colliders at an energy 0.1 – 1 TeV are being developed now in the main high energy centers. Hopefully, in 15–20 years this will be one of the main areas of particle physics.

References

- [1] G. Loew et al., *Intern. Linear Collider Techn. Review Com. Rep.*, SLAC-Rep-471(1996)
- [2] I.Ginzburg, G.Kotkin, V.Serbo, V.Telnov, *Pizma ZhETF*, **34** (1981) 514; *JETP Lett.* **34** (1982) 491.
- [3] I.Ginzburg, G.Kotkin, V.Serbo, V.Telnov, *Nucl. Instr. & Meth.* **205** (1983) 47.
- [4] I.Ginzburg, G.Kotkin, S.Panfil, V.Serbo, V.Telnov, *Nucl. Instr. & Meth.* **219** (1984) 5.
- [5] F.R.Arutyunian and V.A.Tumanian, *Phys.Lett.* **4** (1963)176; R. H. Milburn, *Phys. Rev. Lett.* **10** (1963)75.
- [6] V.Telnov, *Nucl. Instr. & Meth.A* **294** (1990) 72.
- [7] V.Telnov, *Nucl. Instr. & Meth.A* **355** (1995) 3.
- [8] *Proc.of Workshop on $\gamma\gamma$ Colliders*, Berkeley CA, USA, 1994, *Nucl. Instr. & Meth. A* **355** (1995) 1–194.
- [9] *Zeroth-Order Design Report for the Next Linear Collider* LBNL-PUB-5424, SLAC Report 474, May 1996.

- [10] *Conceptual Design of a 500 GeV Electron Positron Linear Collider with Integrated X-Ray Laser Facility* DESY 79-048, ECFA-97-182, e-print: hep-ex/9707017
- [11] V.Berestetskii, E.Lifshits, L.Pitaevskii *Kvantovaya elektrodinamika*, 1989, M.Nauka.
- [12] V.Telnov, *Proc. of ITP Workshop "New modes of particle acceleration techniques and sources"* Santa Barbara, USA, August 1996, NSF-ITP-96-142, SLAC-PUB 7337, Budker INP 96-78, *Phys.Rev.Lett.*, **78**(1997)4757, e-print: hep-ex/9610008.
- [13] For a review, see M. Perry and G. Mourou, *Science*, **264** (1994)917.
- [14] D.Strickland and G.Mourou, *Opt.Commun.* **56** (1985) 219.
- [15] D.Meyerhofer, *Proc.of Workshop on Gamma-Gamma Colliders*, Berkeley CA, USA, 1994, *Nucl. Instr. & Meth.* **A355**(1995)113.
- [16] C.Clayton, N.Kurnit, D.Meyerhofer, *ibid*, p.121.
- [17] V.Telnov, *Proc. of ITP Workshop "Future High energy colliders"* Santa Barbara, USA, October 21-25, 1996, Budker INP 97-47, e-print: physics/9706003.
- [18] V.Telnov, *Proc. the Intern. Conference "Photon 97"*, Egmond aan Zee, The Netherland, May 10-15, 1997, Budker INP 97-54, e-print: physics/9706035.
- [19] P.Chen, V.Telnov, *Phys.Rev.Letters*, **63** (1989)1796.
- [20] V.N.Baier, V.M.Katkov, V.M.Strakhovenko. *Electromagnetic processes at high energy in oriented monocrystals*, Nauka, Novosibirsk, 1989 (in russian).
- [21] G.Kotkin, V.Serbo, e-print: hep-ph/9611345
- [22] V.Telnov, to be published
- [23] N.B. Narozhny, *ZhETF*, v.55 (1968) 714
- [24] V.I.Ritus, *Problems of quantum electrodynamics of intensive field*, Proc. of Lebedev institute, v.168 (1986) p.141 (in russian).
- [25] V.N.Baier, V.M.Katkov, V.N. Fadin. *Radiation of the relativistic electron*, Nauka, Novosibirsk, 1973 (in russian).

Valery Telnov

High Energy Photon-Photon Colliders

Budker INP 97-71

Ответственный за выпуск А.М. Кудрявцев

Работа поступила 16.09. 1997 г.

Сдано в набор 17.09.1997 г.

Подписано в печать 17.09.1997 г.

Формат бумаги 60×90 1/16 Объем 1.4 печ.л., 1.1 уч.-изд.л.

Тираж 100 экз. Бесплатно. Заказ № 71

Обработано на IBM PC и отпечатано на ротапинтере ГНЦ РФ "ИЯФ им. Г.И. Будкера СО РАН", Новосибирск, 630090, пр. академика Лаврентьева, 11.